College of Engineering

ISSN: 1813-162X (Print) ; 2312-7589 (Online)

Tikrit Journal of Engineering Sciences

available online at: http://www.tj-es.com

TJES
Tikrit Journal of Engineering Sciences

Experimental Analysis of Heat Transfer Enhancement and Flow with Cu, TiO_2 Ethylene Glycol Distilled Water Nanofluid in Spiral Coil Heat

Khalid Faisal Sultan *

Electromechanical Engineering Department
University of Technology
Baghdad
Iraq

***Keywords*:**

Nanofluid
ethylene glycol
enhancement
metallic
nano metallic

A R T I C L E I N F O

Article history:

Received 01 June 2014
Accepted 22 February 2017
Available online 30 September 2017

A B S T R A C T

This experimental investigation was performed to improve heat transfer in the heat exchanger (tube of shell and helically coiled (using nanoparticles for turbulent parallel flow and counter flow of distilled water (Dw) and ethylene glycol (EG) fluids. Six types of nanofluids have been used namely: copper – distilled water, copper – distilled water and ethylene glycol, copper – ethylene glycol, titanium oxide – distilled water, titanium oxide – distilled water and ethylene glycol, titanium oxide – ethylene glycol with 0.5%,1%,2%,3% and 5% volume concentration as well as the range of Reynolds number are 4000 – 15000. The experimental results reveal that an increase in coefficient of heat transfer of 50.2 % to Cu – Dw, 41.5% to Cu – (EG + Dw), 32.12 % for Cu – EG , 36.5% for TiO2 – Dw, 30.2 % to TiO2 – (EG + Dw) and 25.5%, to TiO2 – EG . The strong nanoconvection currents and good mixing caused by the presence of Cu and TiO2 nanoparticles. The metal nanofluids give more improvement than oxide nanofluids. The shear stress of nanofluids increases with concentration of nanoparticles in the case of parallel and counter flow. The effect of flow direction is insignificant on coefficient of overall heat transfer and the nanofluids behave as the Newtonian fluid for 0.5%,1%,2%,3% and 5%. Good assent between the practical data and analytical prediction to nanofluids friction factor which means the nanofluid endure pump power with no penalty. This study reveals that the thermal performance from nanofluid Cu – Dw is higher than Cu – (EG + Dw) and Cu – EG due to higher thermal conductivity for the copper and distilled water compared with ethylene glycol.

DOI: http://dx.doi.org/10.25130/tjes.24.3.09

التحليل العملي في تحسينِ انتقال الحرارةِ والجريان للموائع النانوية باستخدام النحاس، وأوكسيد التيتانيوم مع اثيلين كلايكول وماء مقطر في مبادل حراري حلزوني

الخلاصة

تحقيق عملي لتحسين انتقال الحرارة والجريان بواسطة استعمال جزيئات نانوية مثل النحاس وأوكسيد التيتانيوم من خلال مبادل حراري حلزوني مع ماء مقطر واثلين كلايكول وللجريان مضطرب متوازي ومتعاكس. ستّة أنواع مِنْ الموائع النانوية استعملت وهي نحاس- ماء مقطّرَ، نحاس – ماء مقطّرَ وأثيلين كلايكول، نحاس – إثيلين كلايكول ، أوكسيد التيتانيوم – ماء مقطّرَ، أوكسيد التيتانيوم – ماء مقطّرَ وأثيلين كلايكول، أوكسيد التيتانيوم - إثيلين كلايكول مع تراكيز حجميه هي 0.5% , 1%, 2%, 3%, 5%. بينت النتائج العملية ان الزيادة بمعامل انتقال الحرارة كانت كالتالي, 50.2 % Cu – Dw, 41.5% Cu – (EG + Dw), 32.12 % Cu – EG 36.5% TiO2 – Dw , 30.2 % TiO2 – (EG + Dw), 25.5%, TiO2 – EG.وجود الجزيئات النانوية مثل النحاس واوكسيد التيتانيوم يساهم بتوليد تيارات حمل نانوية قوية وخلط جيد الموائع النانوية التي تحتوي جزيئات نانوية معدنية تكون أكثر تحسين في انتقال الحرارة من الجزيئات النانوية التي تحتوي على اكاسيد نانوية. اجهاد القص للموائع النانوية يزداد مع زيادة التركيز الحجمي للجزيئات النانوية ولجريان متوازي ومتعاكس. ولا تأثير لتغير اتجاه الجريان على معامل انتقال الحرارة الكلي وتكون هذه الموائع النانوية هي موائع نيوتنية للتراكيز المأخوذة في الدراسة. وهذه المقالة بينت ايضا ان هناك توافق جيد بين النّتائج التجريبيةِ والتحليلية لمعامل الاحتكاك للموائع النانوية. كما واوضحت هذه الدراسة ان الموائع النانوية لأتسبب جزا بطاقة الضخ. ان الدراسة بينت ان الاداء الحراري للنحاس مع الماء المقطر يكون أفضل من النحاس مع الماء المقطر واثيلين كلايكول وكذلك من النحاس مع اثيلين كلايكول بسبب الموصلية العالية للنحاس والماء المقطر مقارنة مع اثيلين كلايكول.

* *Corresponding author: E-mail* : ksultan61@yahoo.com

Nomenclature

b	coil pitch
D	shell diameter, (m)
d	diameter of the spiral coiled, (m)
De	dean number
DW	distilled water
E	roughness of the test tube
EG	ethylene glycol
f	friction factor
f_c	friction factor of coil
k_n	thermal conductivity of nanofluid, (W/m K)
Pr	Prandl number
R^2	coefficient of determination
RC	curvature radius of the coil
Re	Reynolds number
U_0	overall heat transfer coefficient, (W/m^2 K)

Greek symbols

ΔP	pressure drop, (Pa)
μ_n	dynamic viscosity nanofluid, (N s/m^2)
ρ_n	density of nanofluid, (kg/m^3)
γ	shear rate, (1/s)
ϕ	nanoparticle volume fraction

Subscripts

b	base fluid
c	counter flow
i	inlet
n	nanofluid
p	parallel flow

1. INTRODUCTION

Heat exchangers are used in various applications e.g. heating of thermal oil, generation of steam, plants of thermal processing, processing of food and dairy air conditioning, refrigeration and processes of heat recovery. The advantageous causes of helical coil tubes are high coefficient of heat transfer and small size compared with straight tubes. The cost and efficiency of the heat exchangers are very important factors in industry process; there must be an exact equation to determine the heat transfer. All engineering applications include heat transfer through a fluid medium such as refrigeration, automobiles, power plants and heat exchangers. Heat transfer in fluids, essentially, is convection. However, heat transfer coefficients depend on thermal conductivity of the fluid. To improve its a suspension of solid particles and in general solids thermal conductivity is greater than that of fluids. But the mill and micro sized nanoparticles are liable to plug and deposition in micro channels. On the other hand, nanofluid is on stable suspension at a low concentration of nanoparticles. The improvement of the fluid thermal conductivity is due to disperse in fluid of the conventional heat transfer and occurs without problems as plug and deposition and sedimentation and clogging. Pak and Cho [1], investigated experimentally the turbulent friction and heat transfer behaviors of dispersed fluids (Al_2O_3 and TiO_2 particles suspended in water) in a circular pipe. Lee et al. [2], observed enhancement of thermal conductivity of nanofluids using CuO and Al_2O_3 nanoparticles with water and ethylene glycol compared to base fluids. The thermal conductivities of nanofluids with CuO and Al_2O_3 nanoparticles have been determined experimentally using steady – state parallel – plate technique by Wang et al. [3], for different base fluids such as water, ethylene glycol and engine oil. The thermal conductivity of these nanofluids is increased with increasing volume fraction of the nanoparticles.

Xuan and Li [4], studied the augmentation of thermal conductivity of Cu–water nanofluid for different volume fractions of Cu nanoparticles. Xuan and Roetzel [5], concluded from their findings that the heat transfer enhancement is due to the increase of thermal conductivity and to thermal dispersion which is caused by random motion of the particles that coupled with enhanced thermal conductivity.

Das et al. [6], investigated the variation of the thermal conductivity of a nanofluids (Al_2O_3 – water and CuO–water) with temperature using temperature oscillation technique. They observed that an increase in the thermal conductivity with temperature. Yang et al. [7], measured, experimentally, the convective heat transfer coefficients of several nanoparticles – in – liquid dispersions under a laminar flow in a horizontal tube heat exchanger. Koo and Kleinstreuer [8], showed that the Brownian motion has more impact on the thermal properties of the nanofluid than thermo – phoresis. Herish et al. [9] have conducted an experiment to determine the thermal conductivity of Al_2O_3 – water nanofluid during forced convection in a laminar flow through a circular tube with a constant wall temperature. Recently, Zhang et al. [10], measured the thermal conductivity and thermal diffusivity of Au – toluene, Al_2O_3 – water, TiO_2 – water, CuO water and carbon nanotubes – water nanofluids using the transient short – hot – wire technique. Heat transfers of laminar and turbulent flows in coiled tubes were calculated by Seban and McLaughlin [11]. Regers and Mayhew [12] has been calculated pressure drop and heat transfer that heated helically using a coiled tubes by using steam heat.

This study indicates that failing to in the gain in the wall temperature uniformly because the large core region of the remaining work flow. The objective of this study is to analyze the characteristics of heat transfer and fluid flow in a heat exchanger of spiral tube for both, parallel flow and counter flow configurations using base fluid and nanoparticles. The effects of the nanoparticles concentration and different based fluids such as ethylene glycol, distilled water and ethylene glycol distilled water are investigated.

2. NANOFLUID PREPARATION

The two – steps method was used to prepare nanofluids from base fluid and copper (Cu) or titanium oxide (TiO_2) nanoparticles. Nanoparticles dispersion is in three types of base fluid which are namely: distilled water, ethylene glycol and the mixture of ethylene glycol and distilled water with volume ratio of 60:40. After prepare of the nanofluids and packed in an ultrasonic blender for half an hour to aggregate and disperse of a nanoparticle. The acidic pH is much less than the isoelectric point of these particles, thus ensuring positive surface charges on the particles. The surface enhanced repulsion between the particles producing uniform dispersions through the experiments. An image of a nanofluids containing Cu (50nm) and TiO_2 (50nm) are displayed in Fig. 1.

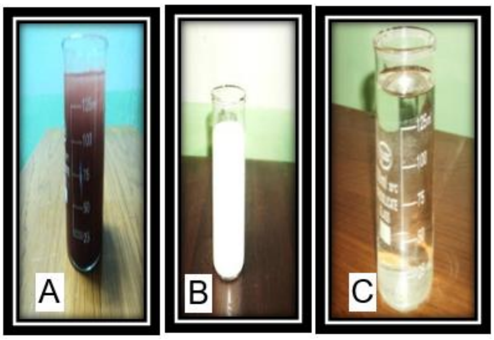

A: Copper–Ethylene glycol
B: Titanium oxide – Ethylene glycol
C: Ethylene glycol

Fig.1. Nanofluids for two types and ethylene glycol.

2.1. Analysis of Geometric Shape for Heat Exchanger

Fig. 2 reveals geometric shape for heat exchanger (spiral coiled and shell heat exchange type).
The curvature ratio of the coil is as follows:

$$\delta = \frac{d}{2\pi Rc} \tag{1}$$

The non – dimensional pitch is as follows:

$$\gamma = \frac{b}{2\pi Rc} \tag{2}$$

Dimensionless factors for heat exchanger in this study are as follows:

$$\left.\begin{aligned} Re_i &= \frac{\rho V_i d_i}{\mu} \quad , \quad Nu_i = \frac{h_i d_i}{k} \\ De &= Re_i \left(\frac{d_i}{2Rc}\right)^{0.5} \quad , \quad He = \frac{De}{(1+\gamma^2)^{0.5}} \end{aligned}\right\} \tag{3}$$

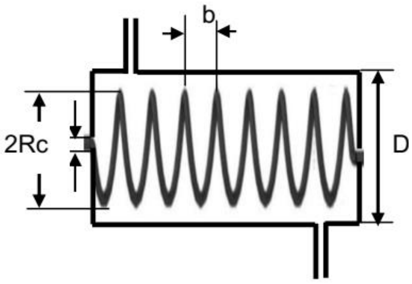

Fig. 2. Geometric shape of heat exchanger.

Mori and Nakayama [13] investigated experimentally a curved pipe with UHF within large *De*. These articles indicate that the two regions of the flow are: BL near the wall and steam condensation on the surface of coil.

Shell – side Reynolds number (Re_o) and Nusselt number (Nu_o) are defined as follows:

$$Re_o = \frac{\rho V_o D_h}{\mu} \quad , \quad Nu_o = \frac{h_o D_h}{k} \tag{4}$$

where: V_o, h_o and D_h are the average velocity, convective heat transfer coefficient and the hydraulic diameter of the shell side respectively.

2.2. Experimental Facility and Procedure

An experimental apparatus and a schematic diagram are used in this work which are shown in Figs. 3 and 4. And a test section is shown in Fig. 5. The heat exchanger is made of Pyrex (soft glass) and the test section is a helical coiled tube of di = 10 mm and do = 12 mm. This helical tube has 34 turns and the coil length is 750 mm. The Pyrex (soft glass) shell has 70 mm inner diameter and 80 mm outer diameter and 1000 mm length. The set–up has helical coiled tube side loop and another side of shell loop. Six types of nanofluids flow in helically coiled tube and this type used copper – distilled water, copper – distilled water and ethylene glycol, copper – ethylene glycol, titanium oxide – distilled water, titanium oxide – distilled water and ethylene glycol, titanium oxide – ethylene glycol. Shell side loop handles hot water.

Fig .3. The experimental system of the convective heat transfers and flow characteristics for the nanofluid.

The studied volume fractions of the nanofluids are (Φ = 0.5%,1%,2%,3% and 5%). Shell side loop consists of a storage vessel of 20 liter capacity with a heater of 3.25 kW, control valve, water pump and a temperature thermostat. The test section consists of a heat exchanger (type shell and spiral tube), pump, needle valve, flow meter of (0.01–3.5) lpm range, cooling unit and a storage vessel of 10 liter capacity. The temperature hot water of the inside the storage vessel (shell side) is maintained via thermostat. The inlet and outlet temperatures of the shell and tube are measured using four T – type thermocouples of 0.15 °C accuracy.

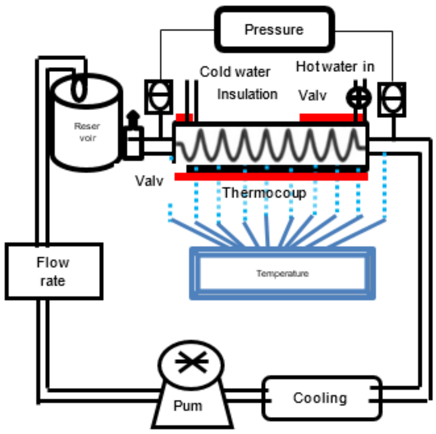

Fig . 4. Schematic diagram of the apparatus.

Fig .5. Test section (Pyrex spiral annulus).

The wall temperatures of the coiled are measured by eight T– type thermocouples. The pressure drop is measured by a pressure gauges that are fixed via the helical tube. The shell is insulated using an Acrylic resin coating the fiberglass sleeve in order to minimize the heat loss from the shell to the atmospheric. The distilled water is tested prior to the nanofluid. And after finishing of construction and calibration of the flow loop then, testing of the loop's functionality for measuring Nusselt number and viscous pressure loss. The numbers of the total tests are 200. At the experiments starts with injecting a hot and then cold water to check there is any leakages. The thermocouples and thermostat are also checked. This six types of nanofluids used in the experiments (Cu –DW,Cu – EG,CU – (EG +DW), TiO_2 – DW, TiO_2 – EG and TiO_2 – (EG+DW)) at 0.5, 1, 2, 3, 5 vol%. The nanofluids of different concentrations would spin through the coil tube while the pump that inside the is switched on when *Dw* reaches the required temperature. Furthermore, the thermostat is attached to *Dw* storage system for this process.

The parallel flow condition is used for flow configuration of first case. Temperatures are recorded at the steady state. This procedure is repeated for all the concentrations. On the other hand, the counter flow was used in the second case, when the flow configuration is changed. The same steps are used in the counter flow. The volume flow rate in the shell has a fixed value of 2.25 lpm while the volume flow rate in the coil tube was varied. The volume flow rate in the coil tube is (0.75-2) lpm. And Reynolds number range is (4000–15000).

2.3. Measurement of the Nanofluid Thermal Properties

The dynamic viscosity (μ) is measured using brook field digital viscometer model DV–E. Figs. 6 and 7 show a comparison between the practical measurement of dynamic viscosity with that obtained from the empirical relation of Einstain, 1956 model [14], Brinkman, 1952 model [15], Wang et al. model [16] and Batchel model [17]. Figs. 8 and 9 represent viscosities of the two types of nanoparticles Cu and TiO_2 with three types of the base fluids DW, EG, EG+DW. The following equipment are used to measure the thermal properties (ρ,μ,K,Cp) respectively. Density is gained by weighing sample and volume, viscometer model (DV – E), Hot Disk thermal constants analyzer (6.1) and specific heat apparatus (ESD – 201). However, the measure density is in a good agreement with the calculated values of that based on [18] theory as shown in Figs. 10 and 11. Figs. 12 and 13 reveal density for the six types of nanofluids. Figs. 14 and 15 indicated the experimental measurements of the thermal conductivity that compared with the thermal conductivity models of many researchers such as Wasp model [19], Hamilton and Crosser [20], Maxwell model [21] and Timo Feeva et al. model [22]. These results showed a good agreement between the Wasp model. Figs. 16 and 17 show the thermal conductivity ratio of the two types of nanoparticles Cu and TiO_2 with three types of the base fluids DW, EG, EG + DW. As well as the measure values for *Cp* compared with the two models of *C*p [23, 24] which are shown in Figs. 18 and 19. The second model showed a good agreement with the measured values. Figs. 20 and 21 depicted the specific heat for the six types of nanofluids**.** The increase in the (μ, ρ, k and C_P) ratios are as follows 10.25%, 5.33%, 16% and 7.2% respectively. This is for the first type of nanoparticle while in the second type of nanoparticles ratios are 8.12%, 3.62%, 11.9% and 2.95% at 5 vol% and 250C as compared with that of the distilled water.

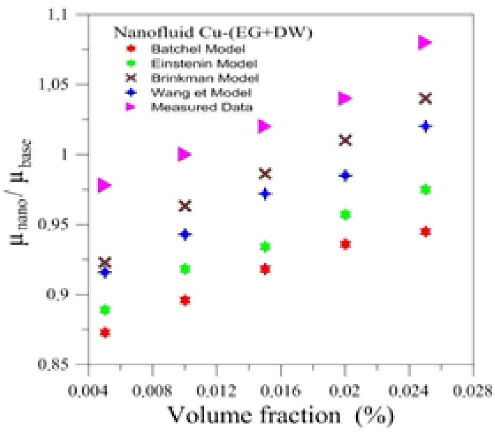

Fig. 6. Viscosity ratio for Cu - (EG+DW).

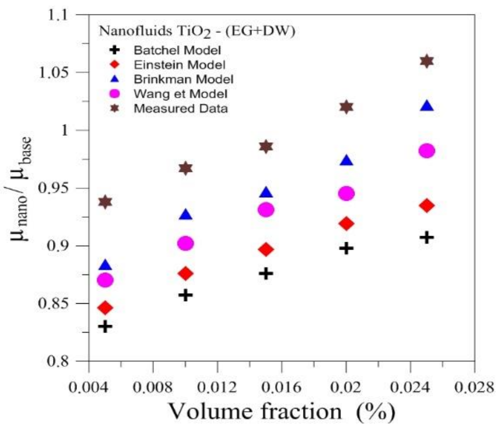

Fig. 7. Viscosity ratio for TiO_2 - (EG+DW).

3. DATA ANALYSIS AND VALIDATION

The heat transfer for the distilled water, ethylene glycol and ethylene glycol. Distilled water are estimated using Eq. (5) and for nanofluid using Eq. (6). Fouling factor is not taken into account.

$$Q_W = m_W c_{PW}(T_{in} - T_{out})_W \quad (5)$$

$$Q_{\mathrm{nf}} = m_{\mathrm{nf}} c_{P\mathrm{nf}}(T_{in} - T_{out})_{\mathrm{nf}} \quad (6)$$

$$q = \frac{Q_{W+}Q_{\mathrm{nf}}}{2} \tag{7}$$

The temperature data and the heat transfer rate were used to calculate the overall heat transfer coefficient, *Uo*, as following [25]:

$$U_o = \frac{q}{A_o\, LMTD} \tag{8}$$

where: A_o surface area; q is the rate of heat transfer; and LMTD is the log of the mean temperature difference.

$$LMTD = \frac{(\Delta T_2 - \Delta T_1)}{\ln\left(\frac{\Delta T_2}{\Delta T_1}\right)} \tag{9}$$

Also

$$Q = h_i A_i (T_W - T_b) \tag{10}$$

$$Nu_i = \frac{h_i d_i}{k_{nf}} \tag{11}$$

where: T_W is the wall temperature, T_b is the bulk temperature, A_i is the inside area and h_i is the inner heat transfer coefficient. U_o and h_i are calculated using Eqs. (8) and (10). Nu_i is calculated using Eq. (11). The coefficient of overall heat transfer is often associated with the inner and the outer heat transfer coefficients using the subsequent equation [25]:

$$\frac{1}{U_o} = \frac{A_o}{A_o\, h_i} + \frac{A_o \ln\left(\frac{D_i}{d}\right)}{2\pi k L} + \frac{1}{h_i} \tag{12}$$

The Nusslet number in the shell side of the heat exchanger is calculate as follows.

$$Nu_o = \frac{h_o D_h}{k_{nf}} \tag{13}$$

where: D_h is the shell hydraulic diameter that calculate as following:

$$D_h = \frac{4(V_{\mathrm{shell}} - V_{\mathrm{tube}})}{\pi(D+d)(L_{\mathrm{shell}} + L_{\mathrm{tube}})} \tag{14}$$

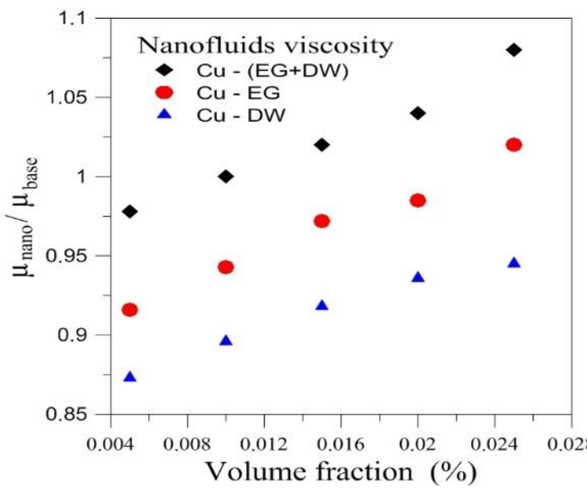

Fig. 8. Three types of viscosity ratio for Cu –DW, Cu - EG and Cu - (EG+DW).

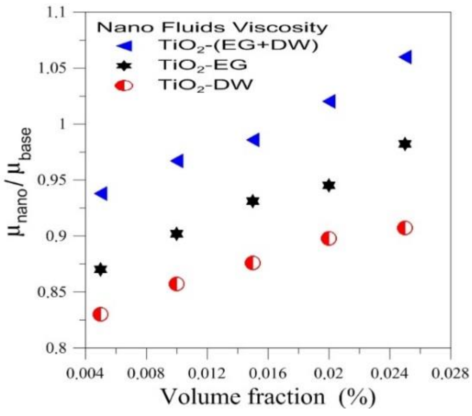

Fig. 9. Three types of viscosity ratio for TiO_2 – DW, TiO_2 – EG and TiO_2 – (EG+DW)

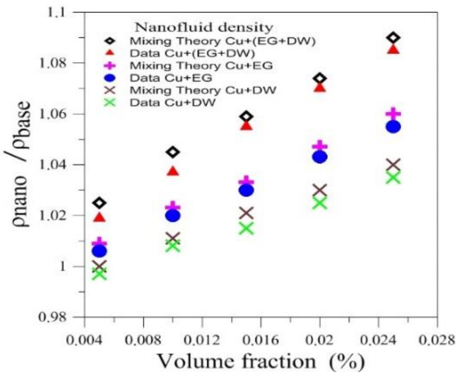

Fig. 10. Comparing the density ratio with the mixing theory for Cu.

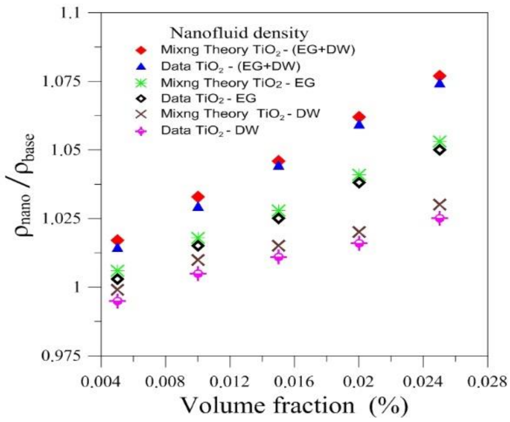

Fig. 11. Comparing density ratio with the mixing theory for TiO_2.

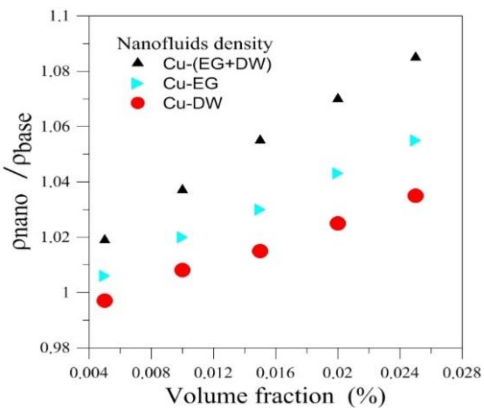

Fig. 12. Three types of density ratio for Cu.

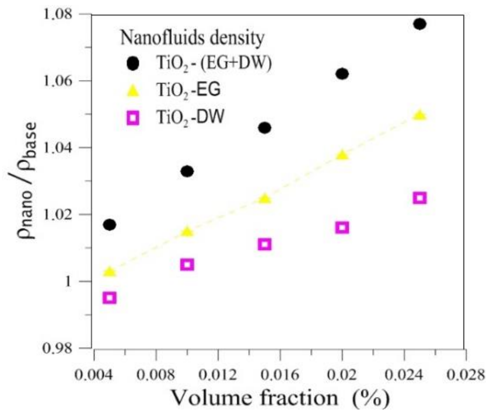

Fig. 13. Three types of density ratio for TiO_2.

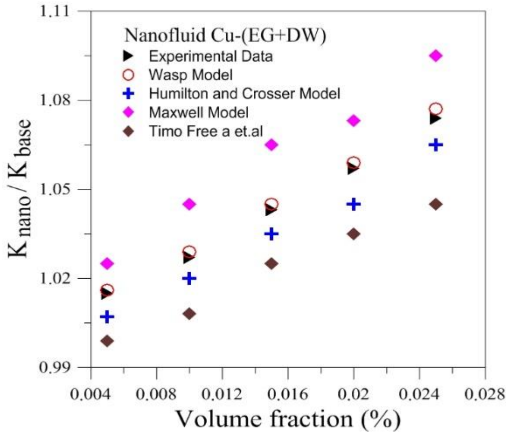

Fig. 14. Thermal conductivity ratio for Cu –(EG+DW).

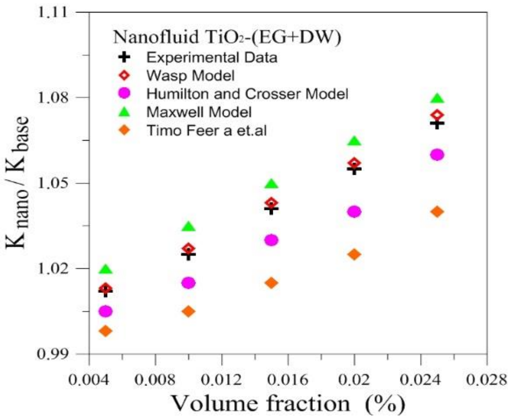

Fig. 15. Thermal conductivity ratio for TiO_2 –(EG+DW).

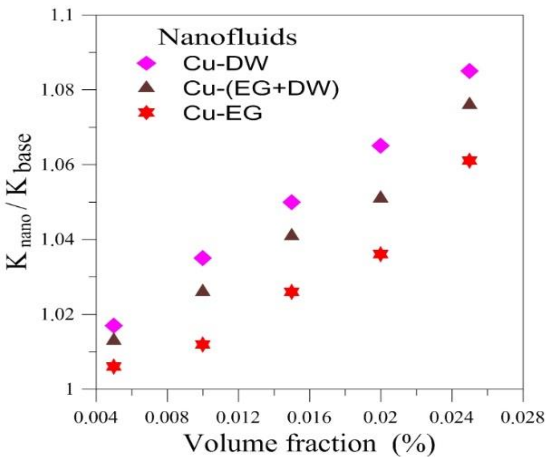

Fig. 16. Three types of thermal conductivity ratio for Cu.

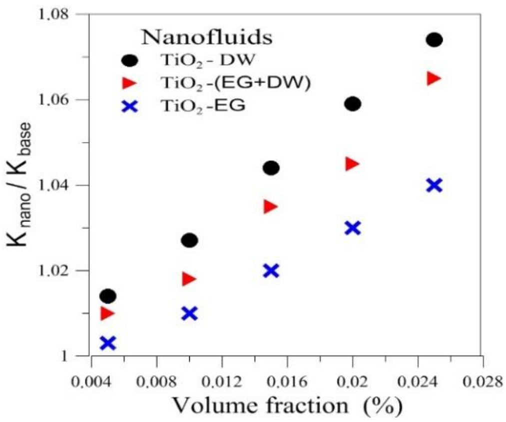

Fig. 17. Three types of thermal conductivity ratio for TiO_2.

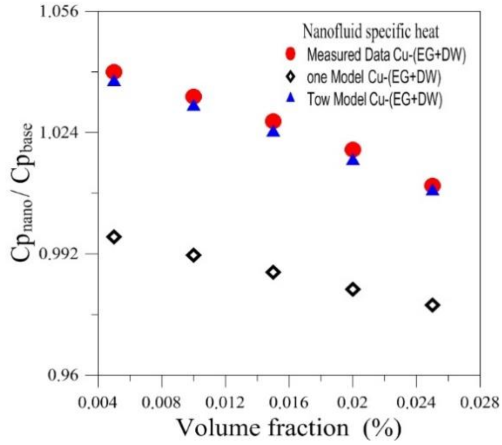

Fig. 18. The specific heat ratio for Cu –(EG+DW).

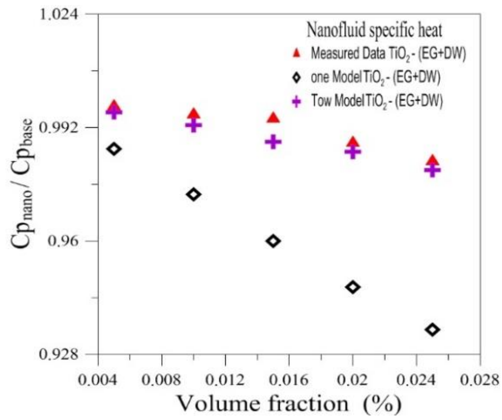

Fig. 19. The specific heat ratio for TiO_2– (EG+DW).

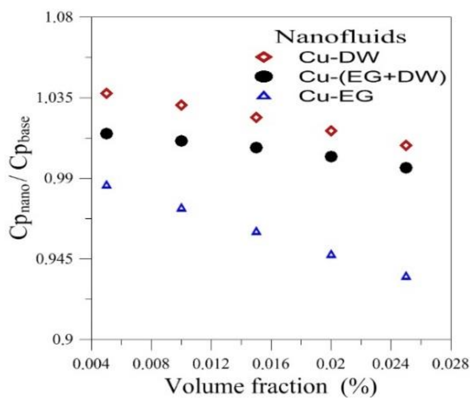

Fig. 20. The three types of the specific heat ratio for Cu.

Similarly, the coefficient of heat transfer, the nanofluids flowing friction factor via the heat exchanger are calculated as follows.

$$f_{nf} = \frac{2D\Delta P_{nf}}{L\rho_{nf} u_{nf}^2} \qquad (15)$$

where: f_{nf} is the nanofluid friction factor, ΔP_{nf} is the nanofluid measured pressure drop, L is the tube length, ρ_{nf} is the nanofluid density, and u_n is the nanofluid mean velocity. The empirical relations between the nanofluids properties were compared with experimental results viscosity, density, thermal conductivity and specific heat.

A. Nanofluid viscosity models

Equation	Ref.
$\mu_{nf} = (1 + 2.5\phi)\mu_{nf}$	[14]
$\mu_{nf} = (1 - \phi)^{-2.5}\mu_{bf}$	[15]
$\mu_{nf} = (1 + 7.3\phi + 123\phi^2)\mu_{bf}$	[16]
$\mu_{nf} = (1 + 2.5\phi + 6.2\phi^2)\mu_{bf}$	[17]

A. Nanofluid density model.

Equation	Ref.
$\rho_{nf} = (1 - \phi)\rho_{bf} + \phi\rho_{bf}$	[18]

B. Nanofluid thermal conductivity models [19–22].

$$k_{nf} = \frac{k_b + (n-1)k_b - (n-1)\left(k_b - k_p\right)\phi}{k_b - (n-1)k_b + \left(k_b - k_p\right)\phi} k$$

$$k_{nf} = \left[\frac{k_b + 2k_b + 2\left(k_b - k_p\right)\phi}{k_b + 2k_b - \left(k_b - k_p\right)\phi}\right] k_b$$

$$k_{nf} = (1 + 3\phi)k_p$$

C. Nanofluid specific heat models.

Equation	Ref.
$c_{nf} = (1 - \phi)c_{bf} + \phi c_P$	[23]
$c_{nf} = \frac{(1-\phi)(\rho c)_{bf} + \phi(\rho c)_P}{\rho}$	[24]

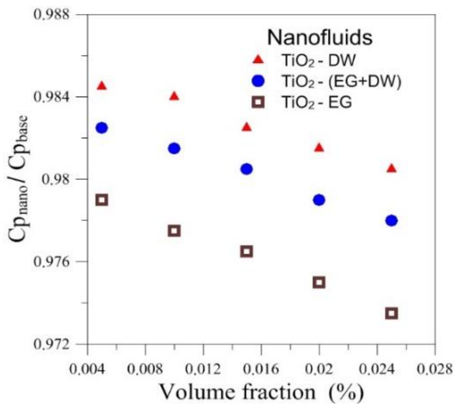

Fig. 21. Three types of the specific heat ratio for TiO_2.

4. RESULTS AND DISCUSSION

In this article the experimental data for the friction factors and coefficient of heat transfer are compared with Shokouhm and Salimpour [26], Salimpour [27] data for a flow in a helical coiled heat exchanger which are defined as follows:

$$Nu_i = 0.112 De^{0.51} \gamma^{-0.37} Pr^{0.72} \qquad (16)$$

$$Nu_o = 5.48 Re^{0.511} \gamma^{0.546} Pr^{0.226} \qquad (17)$$

The friction factor for a turbulent flow in a helical coiled tube, f, is determined as [28].

$$f_c = \frac{7.0144}{Re}\sqrt{De} \qquad (18)$$

Figs. 22 and 23 show a good agreement between the experimental results and the calculated one for using Dw. Figs 24 - 26 show the Uo of the counter flow versus the Uo of parallel flow for three types of nanofluids (Cu –DW,Cu – EG and CU – (EG +DW)). These figures showed a good agreement between data. Uo of the counter flow is 6%–12% greater than that for the parallel flow at 0.5 vol % for three types of nanofluids (Cu –DW,Cu – EG and CU – (EG +DW)). Uo of the counter flow is 25%–52% greater than that for the parallel flow at 5 vol% for the same three types of nanofluids. This means that there insignificant effect of change the heat transfer flow.

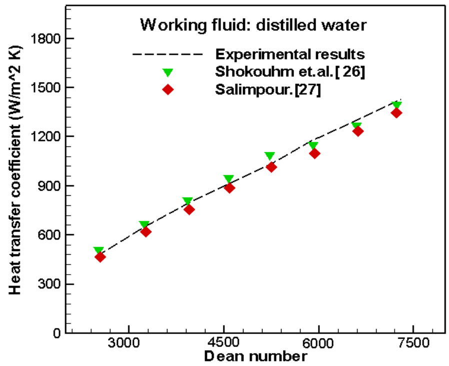

Fig. 22. A comparison between the measured and a calculated heat transfer coefficient that based on [26,27].

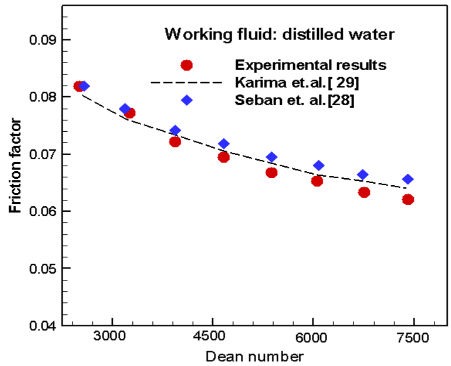

Fig. 23. A comparison between the measured friction factor and the calculated one [28,29].

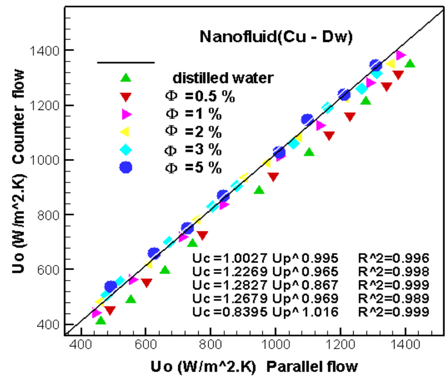

Fig. 24. Overall heat transfer coefficient for two types of flow configuration (counter and parallel) of Cu – DW nanofluid.

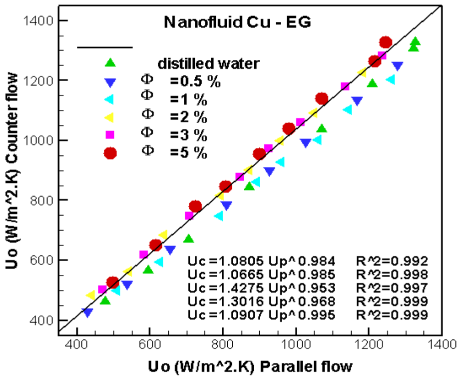

Fig. 25. Overall heat transfer coefficient for two types of flow configuration (counter and parallel) of Cu – EG nanofluid.

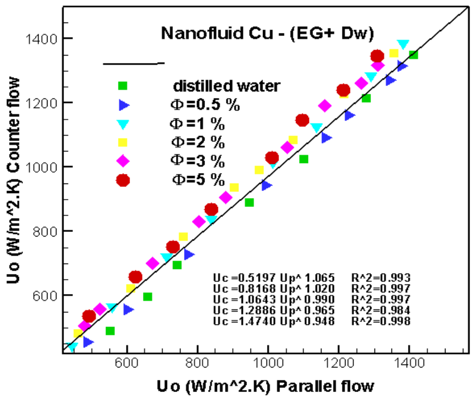

Fig. 26. Overall heat transfer coefficient for two types of flow configurations (counter and parallel) of Cu – (EG+DW) nanofluid.

The reason behind that is: the primary and secondary flow in the tube is perpendicular on the direction of the shell wall. The changing flow direction does not affect Uo. The results from the counter flow Configuration is similar to the that of parallel flow. Heat transfer rates, however, are much higher in the counter flow configuration, due to the increase of the log of the mean temperature difference.

Figs 27 - 38 show the change of Nu_i with De for both, parallel and counter flow. These figures show an insignificant effect on the Nu_i for using nanofluids (Cu – DW,Cu – EG,CU – (EG +DW), TiO_2 –DW, TiO_2 – EG and TiO_2 – (EG +DW)). This is the reason for the flow configuration and h_i. Also the centrifugal force and the secondary flow have an adverse negative effect. And also Nu_i increases with ϕ increse.

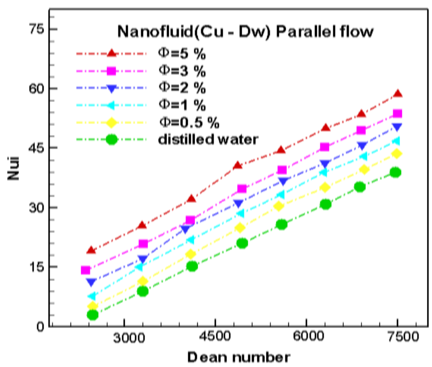

Fig. 27. Variation of Nu_i to nanofluid (Cu-DW) and counter flow.

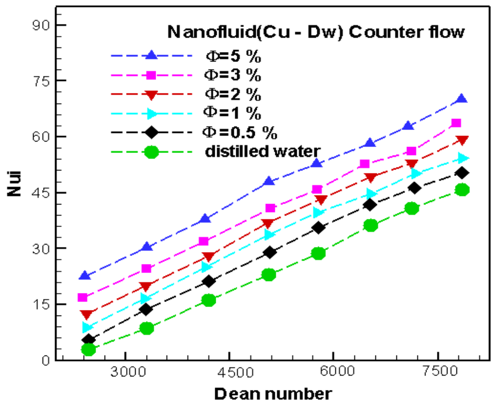

Fig. 28. Variation of Nu_i to nanofluid (Cu-DW) and parallel flow.

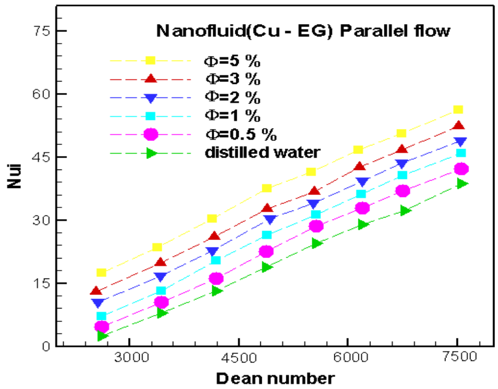

Fig. 29. Variation of Nu_i to nanofluid (Cu–EG) of parallel flow.

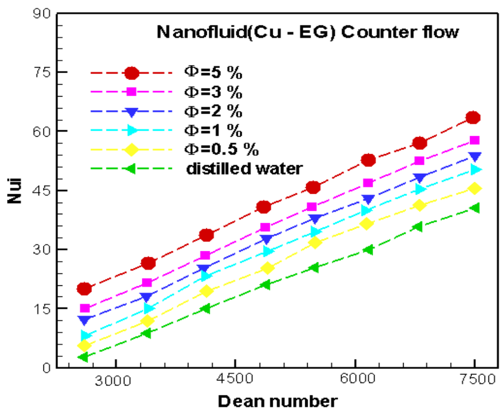

Fig. 30. Variation of Nu_i to a nanofluid (Cu–EG) of counter flow.

In general, the thermal conductivity is proportional to the convective heat transfer. The experimentally determined coefficients of nanofluids friction are shown in Figs. 39 - 44. The experimental friction coefficient results of TiO_2 at 0.5%, 1%, 2%, 3% and 5% particle volume concentration are shown in these figures. Solid line indicates that the experimental results of distilled water and the symbols indicate the nanofluids for turbulent flow. The friction factor of nanofluids (TiO_2 –DW, TiO_2–EG and TiO_2–(EG+DW)) are proportional to the friction factor of the distilled water at low volume fraction concentration of a spiral coil heat exchanger. These figures show that the coefficient of friction of TiO_2

is slightly increased compared with that of the distilled water at high volume fraction concentration due to nanoparticles suspension in Dw. Most of TiO_2 data are located above the line of the distilled water. The friction factor in the spiral coil heat exchanger had an insignificant effect with changing the concentrations of the nanoparticles.

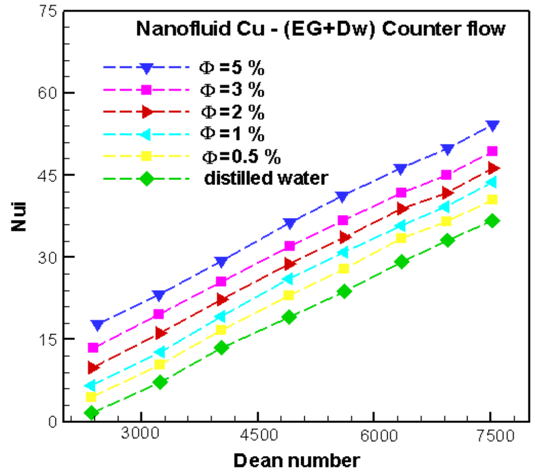

Fig. 32. Variation of Nu_i with nanofluid Cu – (EG + Dw) of counter flow.

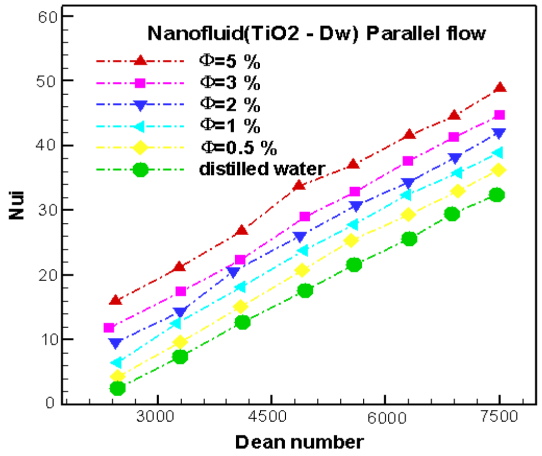

Fig. 33. Variation of Nu_i with nanofluid (TiO_2 –DW) of parallel flow.

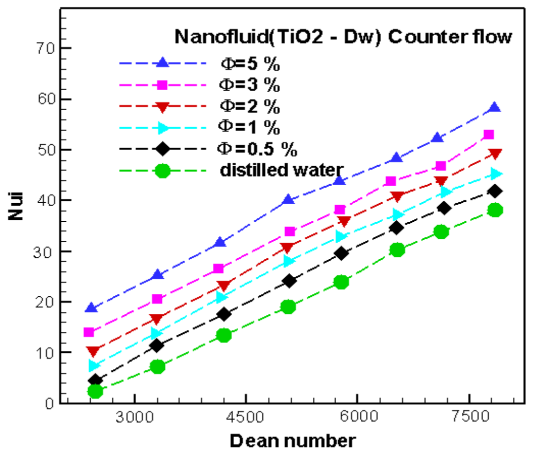

Fig. 34. Variation of Nu_i with nanofluid (TiO_2 –DW) of counter flow.

In this case, there is no need for pumping power. An excess in pressure was noticed when using a nanofluid due to small nanoparticles suspension in Dw which did not change the nanofluid flow behavior. The pressure drop of the base fluid, ethylene glycol is smaller than the base fluid of the distilled water.

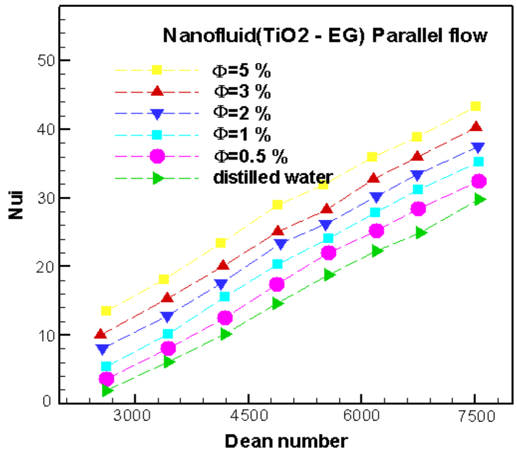

Fig. 35. Variation of Nu_i to nanofluid (TiO_2 –EG) and parallel flow.

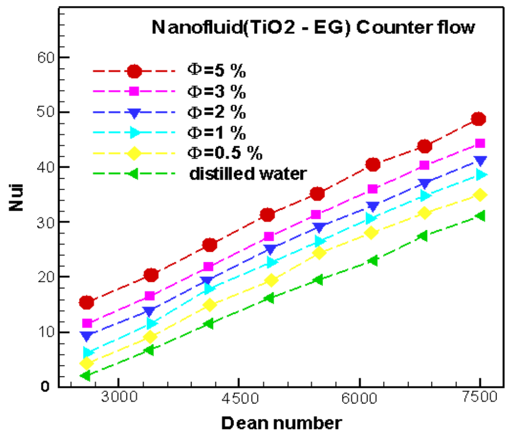

Fig. 36. Variation of Nu_i to nanofluid (TiO_2 –EG) and counter flow.

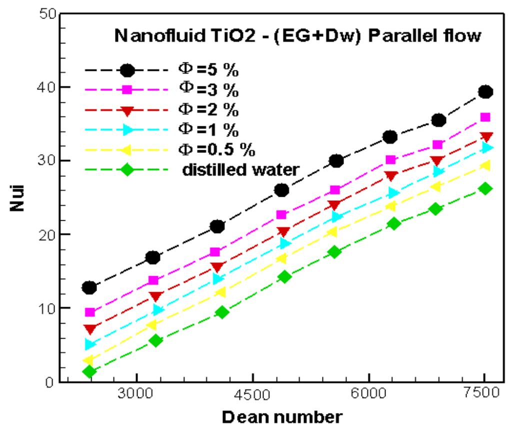

Fig. 37. Variation of Nu_i with nanofluid TiO_2 – (EG + DW) of parallel flow.

Figs. 45 - 50 show the shear stress versus the shear rate for the nanofluids (Cu–DW,Cu–EG and CU–(EG+DW) at 0.5%, 1%, 2%, 3% and 5% particle volume concentration. These figures indicated that the nanoparticles and distilled water are a Newtonian fluid. As well as these figures indicated the shear stress increases with the increase of the shear rate of the nanofluids Cu–DW, Cu–EG and CU–(EG+DW). These figures indicated the flow curve of the nanofluids which is measured using a spiral coil heat exchanger. The shear stress is increased with the volume fraction of parallel and counter flow nanofluids. The use of the nanofluid gives significant higher Nusselt number than the distilled water and ethylene glycol as a based fluid. Also the results indicated that an increase in *h* of 50.2% to Cu–Dw, 41.5% to Cu–(EG+Dw), 32.12% to Cu–EG and 36.5%. to TiO_2 – DW, 30.2 % for TiO_2 – (EG + DW), 25.5%, for TiO_2 – EG.

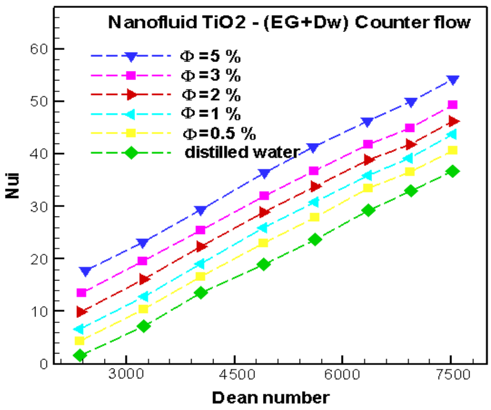

Fig. 38. Variation of Nu_i with nanofluid TiO_2 – (EG + Dw) of counter flow.

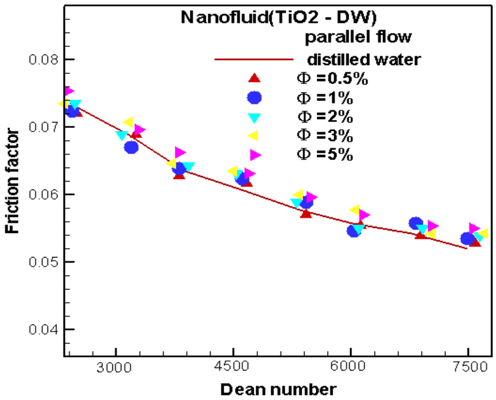

Fig. 39. The friction factor with nanofluid (TiO_2 –DW) of parallel flow.

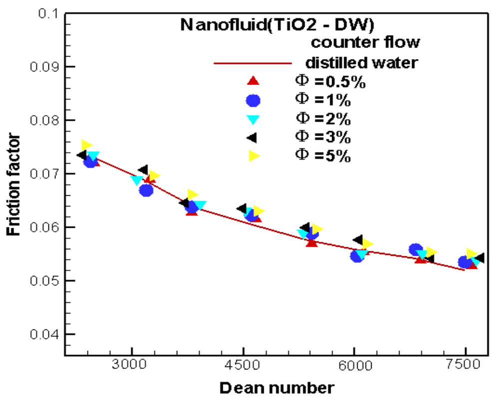

Fig. 40. The friction factor with nanofluid (TiO_2 – DW) of counter flow.

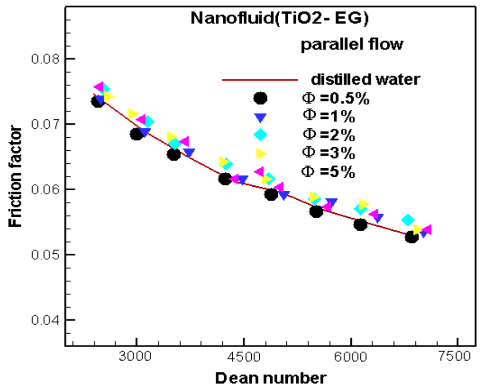

Fig. 41. The friction factor with nanofluid (TiO_2 – EG) of parallel flow.

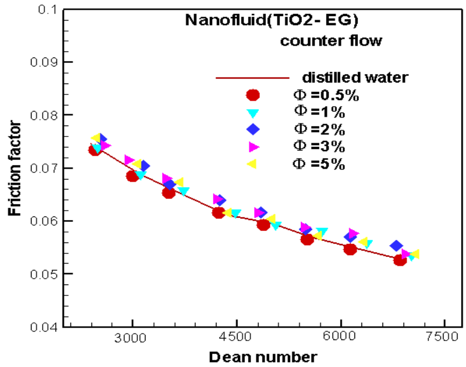

Fig. 42. The friction factor with nanofluid (TiO_2 – EG) of counter flow.

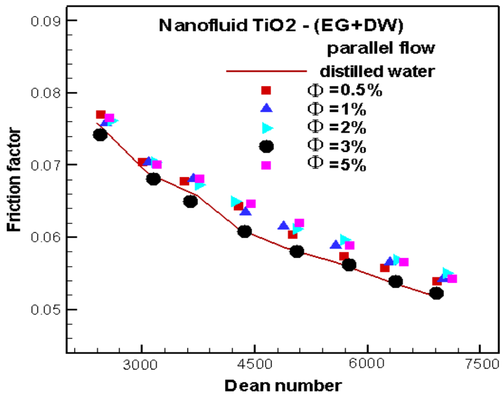

Fig. 43. Variation of friction factor for nanofluid TiO_2 of (EG +DW) for parallel flow.

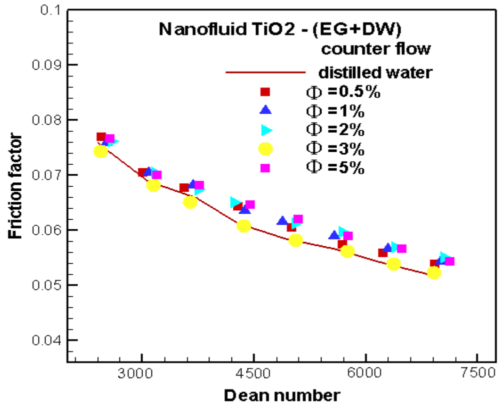

Fig. 44. Variation of friction factor for nanofluid TiO_2 with (EG +DW) for counter flow.

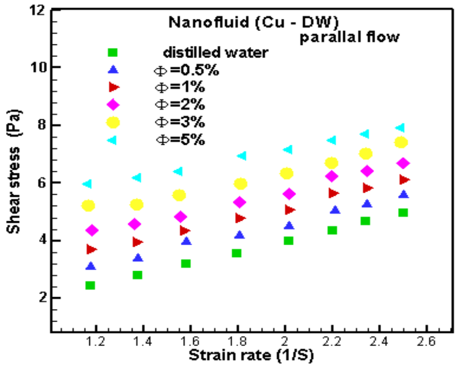

Fig. 45. Shear stress against shear rate for nanofluid (Cu–DW) and parallel flow.

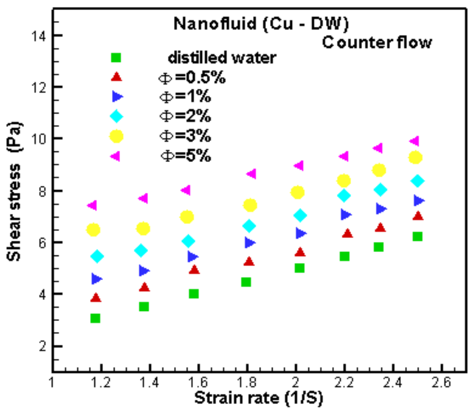

Fig. 46. Shear stress against shear rate for nanofluid (Cu – DW) and counter flow.

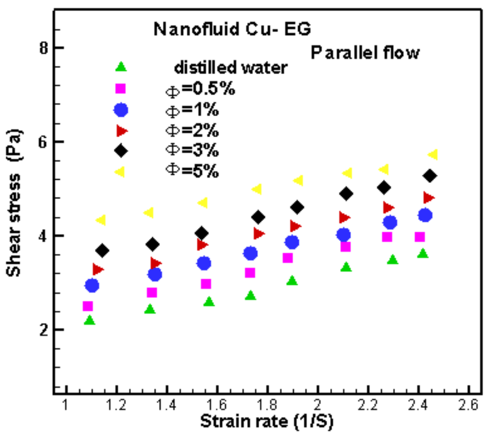

Fig. 47. Shear stress against shear rate for nanofluid (Cu – EG) and parallel flow.

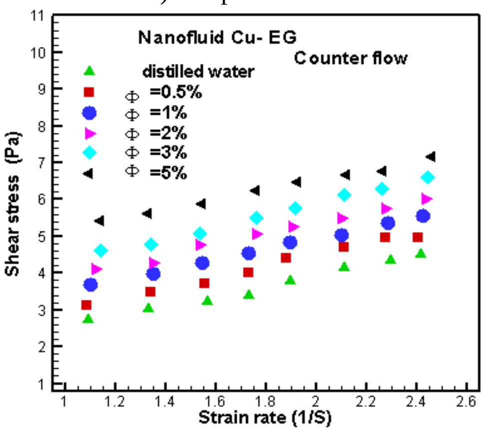

Fig. 48. Shear stress against shear rate for nanofluid (Cu – EG) and counter flow.

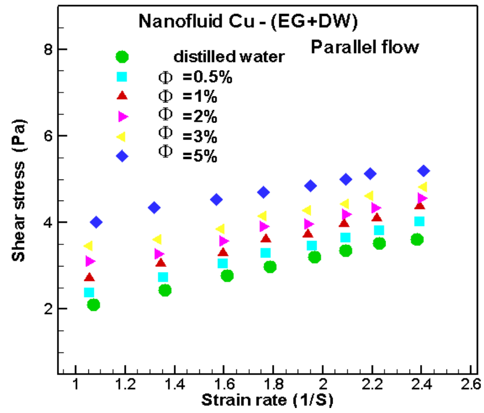

Fig. 49. Shear stress against shear rate for nanofluid Cu – (EG+DW) and counter flow.

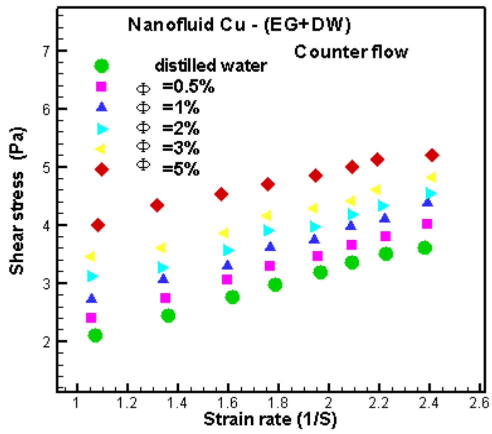

Fig. 50. Shear stress against shear rate for nanofluid Cu–(EG+DW) and parallel flow.

The presence of the nanoparticles (Cu and TiO_2) produces a strong nano convection current and good mixing. The enhancements in the metal nanofluids are better than the oxide metal nanofluids. The coefficient of overall heat transfer is insignificant effect on the flow direction change and the nanofluids behave as the Newtonian fluid for 0.5%, 1%, 2%, 3% and 5%. The experimental results of the frication coefficient of the nanofluid show that there is a good agreement with data of the Colebrook formula. This means that it does not need pumping power and a high value for the pressure purpose drop when using a nanofluid which makes it appropriate for experimental. This study proved that the thermal of the nanofluid Cu–DW is higher than that of Cu–(EG+DW) and Cu–EG nonofluid due to a higher thermal conductivity for the silver and distilled water compared with ethylene glycol.

5. CONCLUSIONS

The main conclusions of the present experimental article are:

1. The type of nanoparticles and base fluid played an important role in the improvement of the heat transfer by the nanofluids.
2. The presence of Cu and TiO_2 nanoparticles attributes to the generation a good mixing.
3. The coefficient of overall heat transfer had insignificant effect on the of the flow direction of the nanofluid (Cu–

DW,Cu – EG and CU – (EG +DW), TiO_2 –DW, TiO_2 – EG and TiO_2 – (EG +DW)) which behaved as a Newtonian fluid for 0.5%,1%, 2%, 3% and 5%.

4. The improvement due to the metal nanofluid is better than that of the oxide metal of nanofluids.
5. The improvement of the nanofluid does not increase the thermal conductivity only but it affects other parameters i.e., viscosity of nanofluid, base fluid.
6. The shear stress of the nanofluids increases with the increasing volume fraction of the nanoparticles of parallel and counter flow.
7. The nanofluid with *Dw* is nearly the same for the pressure drop and friction coefficient while nanofluid with ethylene glycol is smaller than EG. This means that there is no need for pumping power and pressure drop.

REFERENCES

[1] Pak B, Cho Y. Hydrodynamic and heat transfer study of dispersed fluids with submicron metallic oxide particles. *Experimental Heat Transfer* 1998; **11**: 151-170.

[2] Lee S, Choi S, Li S, Eastman JA. Measuring thermal conductivity of fluids containing oxide nanoparticles. *ASME Journal Heat Transfer* 1999; **121**:280–289.

[3] Wang X, Xu X, Choi S. Thermal conductivity of nanoparticle – fluid mixt-ure. *Journal of Thermophysics and Heat Transfer* 1999; **13**: 474–480.

[4] Xuan Y, Li Q. Heat transfer enhancement of nanofluids. *International Journal of Heat and Fluid Flow* 2000; **21**: 58–64.

[5] Xuan Y, Roetzel W. Conceptions for heat transfer correlation of nanofluids. *International Journal of Heat and Mass Transfer* 2000; **43**: 3701–3707.

[6] Das SK, Putra N, Thiesen P, Roetzel W. Temperature dependence of thermal conductivity enhancement for nanofl-uids. *ASME Journal of Heat Transfer* 2003; **125**: 567–574.

[7] Yang Y, Zhang ZG, Grukle AK, Anderson WB, Wu G. Heat transfer properties of nanoparticle-in-fluid disper-sions (nanofluids) in laminar flow. *International Journal of Heat and Mass Transfer* 2005; **48**: 1107–1116.

[8] Koo J, Kleinstreuer C. Impact analysis of nanoparticle motion mechanisms on the thermal conductivity of nanofluids. *International Communications in Heat and Mass Transfer* 2005; **32**: 1111–1118.

[9] Heris SZ, Esfahany MN, Etemad SGh. Experimental investigation of convective heat transfer of Al_2O_3 / water nanofluid in circular tube. *International Journal of Heat and Fluid Flow* 2007; **28**: 203–210.

[10] Zhang X, Gu H, Fujii M. Effective thermal conductivity and thermal diffusivity of nanofluids containing spherical and cylindrical nanoparticles. *Experimental Thermal and Fluid Sciences* 2007; **31**: 593–599.

[11] Seban RA, McLaughlin EF. Heat transfer in tube coils with laminar and turbulent flow. *International Journal of Heat and Mass Transfer* 1963; **6**: 387–395.

[12] Regers GFC, Mayhew YR. Heat transfer and pressure loss in helically coiled tubes with turbulent flow. *International Journal of Heat and Mass Transfer* 1964; **7**: 1207–1216.

[13] Mori Y, Nakayama W. Study on forced convective heat transfer in curved pipe. *International Journal of heat and Mass Transfer* 1965; **8**: 67–82.

[14] Einstein A. Investigation on the theory of Brownian motion. Dover; New York: 1956.

[15] Binkman HC. The viscosity of concentra-ted suspensions and solution. *The Journal of Chemical Physics* 1952; **20** (4): 571.

[16] Wang X, Xu X, Choi S. Thermal conductivity of nanoparticle – fluid mixture. *Journal of Thermophysics and Heat Transfer* 1999; **13**: 474–480.

[17] Batchelor GK. The effect of Brownian motion on the bulk stress in a suspension of spherical particles. *Journal of Fluid Mechanics* 1977; **83** (1): 97-117.

[18] Smith JM, Van Ness HC. Introduction to chemical engineering thermodynamic. McGraw-Hill: New York; 1987.

[19] Wasp EJ, Kenny JP, Gandhi RL. Solid – liquid slurry pipeline transportation, bulk materials handling. Transtechnology Publications: Germany;1999.

[20] Hamilton RL, Crosser OK. Thermal conductivity of heterogeneous two-component systems. *Industrial & Engineering Chemistry Fundamentals* 1962; **1** (3): 187-191.

[21] Maxwell JC. A treatise on electricity and magnetism. 2nd ed. Clarendon Press Oxford: UK;1981.

[22] Timofeeva EV, et al. Thermal conductivity and particle agglomeration in alumina nanofluids. Experiment and Theory. *Physical Review E Journal* 2007; **76** (6): 16-23.

[23] Xuan Y, Roetzel W. Conceptions for heat transfer correlation of nanofluids. *International Journal of Heat and Mass Transfer* 2000; **43**: 3701–3707.

[24] Pak BC, Cho YI. Hydrodynamic and heat transfer study of dispersed fluids with sub micro metallic oxide particles. *Experimental Heat Transfer* 1998; **11**: 151-170.

[25] White FM. Heat transfer. Addison–Wesley Publishing Company Inc.: New York;1984.

[26] Shokouhm H, Salimpour MR, Akhavan MA. Experimental investigation of shell and coiled tube heat exchangers using Wilson plots. *International Communications in Heat and Mass Transfer* 2008; **35**: 84–92.

[27] Salimpour MR. Heat transfer characteristics of a temperature–dependent property fluid in shell and coiled tube heat exchangers. *International Communications in Heat and Mass Transfer* 2008; **35**: 1190–1195.

[28] Seban RA, Mclauchlin EF. Heat transfer in tube coils with laminar and turbulent flow. *Heat Mass Transfer* 1962; **6**: 387–395.

[29] Amori KE, Sherza JS. An investigation of shell–helical coiled tube heat exchanger used for solar water heating system. *Innovative Systems Design and Engineering* 2013; **4** (15): 78-90.